Supplementary Material for

A Triarylmethyl Spin Label for Long-Range Distance Measurement at Physiological Temperatures Using T_1 Relaxation Enhancement

Zhongyu Yang,[1†] Michael D. Bridges,[1] Carlos J. López,[1] Olga Yu. Rogozhnikova,[2,3] Dmitry V. Trukhin,[2,3] Evan K. Brooks,[1] Victor Tormyshev,[*,2,3] Howard J. Halpern,[*,4] and Wayne L. Hubbell[*,1]

1. Jules Stein Eye Institute and Department of Chemistry and Biochemistry, University of California, Los Angeles, Los Angeles, CA, 90095
2. N.N. Vorozhtsov Novosibirsk Institute of Organic Chemistry, Novosibirsk 630090, Russia
3. Novosibirsk State University, Novosibirsk 630090, Russia
4. The Center for EPR Imaging in vivo Physiology, Department of Radiation and Cellular Oncology, University of Chicago, Chicago, IL 60637

†*Present address*: Department of Chemistry and Biochemistry, North Dakota State University, Fargo, ND, 58102

1. **TAM synthesis.**

Tris(8-carboxy-2,2,6,6-tetramethylbenzo[1,2-*d*;4,5-*d'*]bis[1,3]dithi-ol-4-yl)methyl (**1**, Finland trityl, *Scheme 1 – main text*) was prepared by the recently published literature method [1].

S-3-hydroxypropyl methanesulfonothioate (3). A solution of 3-bromopropan-1-ol (**2**) (0.417 g, 3 mmol), sodium methanethiosulfonate (0.523 g, 3.9 mmol) in anhydrous DMF (4 mL) was stirred under argon at 70^{o}C for 44 h. The mixture was concentrated in vacuo. The residual DMF was removed by suspending the crude product with toluene followed by evaporation of solvents (3 x 5 mL of toluene). Column chromatography on silica gel (hexane/ethyl acetate 1:1 v/v, then ethyl acetate afforded a title alcohol **3** as a pale-yellow syrup with characteristic onion smell. Yield: 0.485 g, 94%. ^{1}H NMR (400 MHz, $CDCl_3$): δ = 1.97 (m, 2H, $CH_2CH_2CH_2$), 2.55 (bs, 1H, O*H*), 3.28 (t, 2H, *J* = 7.0 Hz, SCH_2), 3.32 (s, 3H, SO_2CH_3), 3.73 (t, 2H, *J* = 5.6 Hz, OCH_2). ^{13}C NMR (100 MHz, $CDCl_3$): δ = 31.56 ($CH_2CH_2CH_2$), 32.13 (SCH_2), 50.42 (SO_2CH_3), 59.99 (OCH_2). IR (thin film): $\tilde{\nu}$ = 3541 (m), 3395 (m), 3028 (w), 3009 (w), 2928 (m), 2884 (w), 1410 (w), 1312 (vs), 1130 (vs), 1049 (m), 959 (m), 748(m), 555 (s), 482 (m).

Methanethiosulfonate derivative of Finland trityl (TAM-MTS, 4). A mixture of Finland trityl **1** (0.200 g, 0.20 mmol) and dry triethylamine (0.091 g, 0.90 mmol) in freshly distilled anhydrous chloroform (0.50 mL) was stirred at room temperature for 1 h. Crystalline N,N'-bis(2-oxo-3-oxazolidinyl) phosphinic chloride (BOP-Cl, 0.058 g, 0.22 mmol) and solution of alcohol **3** (0.044 g, 0.26 mmol) in anhydrous chloroform (0.20 mL) were added dropwise over 5 min to resulting deep reddish-brown solution was added a solution of 4-dimethylaminopyridine (DMAP, 0.005 g, 0.04 mmol) in chloroform (0.2 mL). The mixture, which slowly turned to deep green, was stirred under argon at 30^{o}C for 48 h, and then transferred to a 50 mL conical flask. Water (10 mL), THF (5 mL) and sodium bicarbonate (0.93 g, 11.1 mmol) were added, and resulting heterogeneous mixture was vigorously stirred for 20 min. The water phase was acidified with 0.2 M aqueous HCl to pH 3, after which the mixture was extracted with THF (3 x 10 mL). The combined organic extract was filtered and concentrated in vacuo. Column chromatography on silica gel (DCM, then DCM/methanol from 30:1 to 10:1 v/v) gave the trityl **4** as a brownish-black precipitate. Yield: 0.051 g, 22%.

HR MS (ESI, *m*/*z*): 1149.921 (measured), 1149.9288 (calculated for $C_{44}H_{46}O_8S_{14}$ $[M-H]^-$). IR (KBr): $\tilde{\nu}$ = 2955 (m), 2920 (m), 2855 (m), 1703 (m), 1574 (s), 1487 (m), 1450 (m), 1385 (s), 1315 (s), 1234 (vs), 1167 (m), 1132 (m), 1113 (m), 731 (w), 555 (w) cm^{-1}. ESR spectrum for 0.60 mM solution in methanol: singlet, linewidth 758 mG, g = 2.0058 (*used in all distance measurement calculations below, as 'g_s'*).

2. T4L sample preparation.

Mutants of 23L/131C, 37L/76C, and 135L/76C, where "L" indicates a GGGHG pentapeptide loop, were prepared as described before [2]. Briefly, the DNA of these mutants were generated by QuikChange site-directed mutagenesis of the pET11a-T4L genetic construct containing the pseudo-wild-type mutations C54T and C97A [3,4], followed with verification of each mutation by DNA sequencing [5]. These mutants of T4L were expressed, purified, and then desalted (to remove DTT) into a buffer suitable for spin labeling (referred to hereon as "spin labeling buffer") containing 50 mM MOPS and 25 mM NaCl at pH 6.8) using previously reported procedure [3]. For these proteins to be tethered directly to CNBr activated sepharose, the cysteine residues were protected from reaction with the activated Sepharose by reaction with a 10 fold molar excess of *S*-(2,2,5,5-tetramethyl-2,5-dihydro-1H-pyrrol-3-yl) methyl methanesulfonothioate (MTSL, a generous gift from Prof. Kalman Hideg) 4°C overnight (yielding R1). Excess MTSL was removed using an Amicon spin concentrator (Millipore, 10,000 MWCO, 50 ml).

The mutant containing the unnatural amino acid at site 65 (23L/65*p*-AcF/131C) was prepared as described by López et al. [6]. Briefly, for generation of T4L containing *p*-AcF, the amber (TAG) stop codon was introduced at site 65 using the QuikChange Site-Directed mutagenesis method (Stratagene). For unnatural amino acid incorporation in *E. coli*, two plasmids are required, one for expression of the gene of interest (containing the TAG codon) and a second that contains the orthogonal tRNA and aminoacyl-tRNA synthetase pair. For introduction of *p*-AcF, the p-Ultra I-*p*-AcF plasmid was used. For protein expression, *E. coli* BL21(DE3) cells (Stratagene) were cotransformed with the pET11a vector containing T4L and the p-Ultra I-p-AcF vector, and then plated onto LB-agar plates containing ampicillin and chloramphenicol for selection (100 μg/mL ampicillin and 34 μg/mL chloramphenicol). After overnight incubation at 37°C, single colonies were inoculated into 20 mL of starter LB medium containing the aforementioned antibiotics and then allowed to grow overnight at 37°C in a shaking incubator. The following day, the starter culture was inoculated into 3 L of LB medium containing the aforementioned antibiotics and allowed to grow at 37°C in a shaking incubator to an OD_{600} of 1.0, then *p*-AcF (obtained from SynChem; Elk Grove Village, IL) was added to a final concentration of 2 mM; after another 30 min. shaking, protein expression was induced with 1 mM isopropyl-β-D-thiogalactopyranoside. The culture was incubated overnight at 30°C in the shaking incubator and then harvested by centrifugation. Protein purification and spin labeling were performed as described above.

3. Protein immobilization on CNBr activated solid support via random attachment.

CNBr-activated sepharose beads were purchased from Sigma-Aldrich, and activated as described previously [3]. Typical bead volume for each sample was ~100 μl suspended in ~0.5 ml of spin labeling buffer. Approximately 1.0 mg of protected protein (50 nmol, prepared as described above) was added to the beads/buffer mixture (final expected protein concentration should be ~500 μM). After incubating 2 hrs at room temperature, samples were centrifuged at 3000 × g for 1 min. The supernatant was removed and concentrated using the spin concentrator (Millipore, 10,000 MWCO, 500 μL). The unbound protein in the supernatant was determined by the absorbance at 280nm (ε_{280} = 24,750 $cm^{-1}M^{-1}$); essentially all protein was coupled, leading to a final protein concentration on beads of ~ 500 μM.

The CNBr activated beads with labeled protein were resuspended using 0.5 ml of the spin labeling buffer. Dithiothreitol was added to a final concentration of 5 mM and allowed to incubate for 1 hr at room temperature to remove the R1 group. DTT and products were removed by washing with spin labeling buffer 6 times (for each wash, the beads were resuspended in 1 ml buffer, centrifuged at 3000 × g for 1 min and the supernatant removed). CW EPR spectra were used to confirm that there was no R1 spin label in the bead sample. The TAM-MTS reagent **4** (Scheme 1) was then added to each sample with a molar ratio of about 3:1 (TAM-MTS to free cysteine) and allowed to react for 12-16 hrs at 4°C. Unreacted TAM-MTS was removed by washing 3 times with the spin labeling buffer.

4. Biotinylation and site-specific attachment of T4L 23L/65*p*-AcF/131C.

Purified and spin-labeled mutant T4L 23L/65*p*-AcF/131C was exchanged to a buffer consisting of 50 mM sodium phosphate, 25 mM NaCl at pH 4.0 and then incubated with 10-fold molar excess of a freshly made solution of N-(aminooxyacetyl)-N'-(D-biotinoyl) hydrazine trifluoroacetic acid salt (Invitrogen). The mixture was incubated overnight at 37°C with nutation to yield the biotinylated protein. Excess reagent was removed by three 15-ml washes with PBS buffer (100 mM phosphate, 150 mM NaCl) at pH 7.2, using a 15-ml Amicon Ultra concentrator (10 kDa MWCO).

For site-specific tethering of biotinylated T4L to high-capacity streptavidin beads (Thermo Scientific), the desired quantity of Strepavidin beads was equilibrated in PBS buffer (pH 7.2) and washed three times by centrifugation with a 5-fold excess of the same buffer. After the final wash and removal of the supernatant, the biotinylated protein was added to the beads in an amount equivalent to the stated

capacity of the resin (10 mg/ml) and the suspension was mixed at room temperature for at least 2 hours at room temperature or at 4°C overnight. The supernatant was removed and the beads washed with buffer consisting of 50 mM MOPS, 25 mM NaCl at pH 6.8 prior to EPR measurements. The coupling efficiency was determined from the A_{280nm} of the supernatant and washes compared to that of the protein solution added to the beads.

5. Labeling efficiency.

Labeling efficiency with TAM-MTS was characterized using the 4-PyDS titration approach [7-9]. Briefly, ~100 µL CNBr-Sepharose beads with bound protein or 150 uL Streptavidin coated beads with bound protein are suspended in 1 mL spin labeling buffer. Each bead suspension was then divided into two aliquots (each containing 0.5 mL buffer and 50 uL CNBr beads or 0.75 mL buffer and 75 uL Streptavidin coated beads). One aliquot of each sample was treated with 4-PDS (2.5 uL at 100 mM concentration) at room temperature for ~10 mins on a shaking platform. The UV 324 nm of the supernatant of the mixture was then recorded to quantify the amount of total active protein thiol groups. The other aliquot of beads sample was reacted with the TAM labeling reagent (TAM-MTS) on a 3 to 1 TAM-MTS-to-protein ratio at 4°C overnight. The reacted beads were then washed three times with spin labeling buffer, and resuspended in 0.5 mL buffer. This sample was then treated with 4-PDS (2.5 uL at 100 mM concentration) for 10 mins at room temperature on shaker. The UV 324 nm of the supernatant of the mixture was then recorded to quantify the amount of unreacted, active thiol groups.

6. Continuous Wave EPR Spectroscopy.

To prepare the samples for recording the CW spectra in Figure 3 of the main text, T4L 76C was purified and desalted as described above, followed by dilution to 100 µM, and spin labeling with TAM-MTS in aqueous solution at a 3:1 spin-label to protein ratio at room temperature for two hours. Approximately 50% of the protein was lost at this step as aggregates (removed by centrifugation and filtration), and excess spin labeling reagent was removed with repeated rinses with fresh buffer in an Amicon spin concentrator (Millipore, 10,000 MWCO, 50 ml), and concentrated to 200 µM. This stock was divided in three parts: one aliquot was reacted with CNBr-activated Sepharose, one was diluted by half with buffer to yield 100 µM concentration, and the third was diluted by half with a 60% *w/w* sucrose solution to yield a concentration of 100 µM in 30% *w/w* sucrose solution. The TAM-MTS sample was simply diluted in the above MOPS buffer to a concentration of 100 µM. Approximately 15 µL of sample was loaded into a gas-permeable 4-methylpent-1-ene (TPX) capillary tube (0.70 mm i.d./1.25 mm o.d.; Molecular Specialties, Inc., Milwaukee), which was installed in a Varian E-109 spectrometer fitted with

a E-231 cavity resonator, which operates with a rectangular TE_{102} mode. Nitrogen gas was flowed through the resonator to deoxygenate the samples for 15 minutes prior to and during data acquisition.

All continuous wave (CW) EPR spectra were obtained with a low observe power of 10 μW to minimize power saturation broadening. All spectra were obtained with modulation frequency of 100 kHz, but with differing modulation amplitudes: 0.02 G for TAM-MTS and 76TAM1 in buffer, 0.04 G for 76TAM1 in sucrose, and 0.10 G for 76TAM1 on Sepharose; in each case these modulation amplitudes are more than an order of magnitude less than the linewidths observed and so are not expected to contribute to spectral line broadening.

7. Saturation Recovery EPR Spectroscopy.

SR data were acquired using a Bruker E580 spectrometer equipped with a loop-gap resonator and a Stanford Research preamplifier as described before [10]. Each sample with a typical bead volume of 2-3 μL was loaded into a TPX capillary with an inner diameter of 0.6 mm (Molecular Specialties Inc., Milwaukee, WI). Before each measurement, the sample was equilibrated at 298 K under nitrogen flow to remove oxygen using a Bruker temperature controller. Both the saturation and observe pulses were set to the maximum absorbance of the TAM absorbance spectrum. The saturation pulse length was 8 μs, with an incident power of 250 mW. The long saturation pulse was employed to minimize the effects of spectral diffusion [11]. Saturation recovery was monitored with observe powers of 200, 100 and 50 μW so that copper-free T_1 values obtained from our fitting procedure (described below) could be extrapolated to zero observe power to determine the intrinsic T_1 of the sample [12]. The total number of acquisitions for each recovery curve was 2.1 million and each spectral acquisition was repeated 3-4 times with the results averaged.

8. DEER EPR Spectroscopy.

All DEER experiments were performed at Q band using the Bruker E580 at 80 K as described in a recent work [13]. The standard DEER pulse sequence was used, where the $\pi/2$ and π pulses were 16 and 32 ns, respectively [13], with a step size of 16 ns. The pump and the observe pulses were adjusted to excite proper spins depending on different samples (see Results and figure legends). DEER data were analyzed using LongDistances [14]. To obtain the field-swept electron spin echo spectrum (FS-ESE), the size of the standard Hahn echo was monitored as a function of magnetic field. The pulse lengths were kept the same as in DEER experiment. All FS-ESE experiments were carried out at Q band.

9. Raw data and data analysis of TAM-labeled samples in this work.

For proteins immobilized on solid support, the spin lattice relaxation depends on the orientation of the Cu^{2+}/TAM1 interspin vector with respect to the applied magnetic field described by an angle θ according to Equation 1 of the main text. The time dependence of the experimental relaxation curve is then determined by contributions from each orientation weighted by $sin\,\theta$ as described by Hirsch *et al.* [15] according to,

$$S_{Cu}(t) = 1 - \left[\int \exp\left(-t\left(\frac{1}{r^6}\right)\frac{3g_s^2 g_f^2 \beta_e^4}{4\hbar^2}\left[\left(\frac{1}{6}\right)\frac{T_{2f}}{1+(\omega_f-\omega_s)^2 T_{2f}^2}\left(1-3cos^2\theta\right)^2 + \frac{3T_{1f}}{1+\omega_s^2 T_{1f}^2} sin^2\theta cos^2\theta + \right.\right.$$

$$32T2f1+\omega f+\omega s2T2f2sin4\theta sin\theta d\theta \times \exp -t1T1s0$$

(*Equation S1)*

where $S_{Cu}(t)$ is the time-dependent amplitude of the relaxation curve obtained for copper-bound samples. For samples absent of Cu^{2+}, the relaxations are orientation independent and fit with a single exponential characterized by the copper-free T_1 of TAM1, T_{1s}^0, i.e.,

$$S_{int}(t) = 1 - \exp\left(-t\left[\frac{1}{T_{1s}^0}\right]\right) \qquad \textit{(Equation S2)}$$

In practice, the first 7 μs of the ~70 μs relaxation curves were found to be contaminated by signals possibly arising from incomplete saturation [16] and/or imperfect phase cycling or off-resonance subtraction as discussed in Sato *et al*. [17] so these early time points were removed before analysis. To extract the interspin distance, r, the experimental relaxation curves for the copper-free and copper-bound samples were simultaneously fit in a least-squares sense to the above expressions with T_{1s}^0 and r as variable parameters (along with the experimental amplitudes and offsets for both traces). The integration is performed numerically over $\theta = 0$ to 90° with 90 orientations. A Labview program was written to perform the fitting, and reports the best fit values and errors and plots the data, best-fit line, and residual for each data set (plotted below for the four samples studied as Figures S1-S4).

The true, or intrinsic, T_{1s}^0 values for TAM1 in the absence of Cu^{2+}, and thus the apparent relaxation in the presence of Cu^{2+}, can only be determined at very low observe powers, because application of an observe microwave field shortens T_1 [16]. This is illustrated in Figure S5 for the relaxation times obtained by fitting the data as described above; inverse T_{1s}^0 values are linearly extrapolated to zero observe power to determine an intrinsic value.

Note that the enhanced relaxation of T_1 due to Cu^{2+} in copper-bound samples is expected to be independent of observe power, as demonstrated by Yin and Hyde [12]. To test this, the values of r determined by the above fitting procedure at observe powers of 200, 100 and 50 μW were compared. The values varied by ≈10%, but the variation was not systematic, i.e., the values did not regularly increase or decrease with power in all samples; the r values reported in Table 1 of the text are the error-weighted average values. Experimental and extrapolated T_{1s}^0 values are provided in Tables S1-S4, as are experimental and averaged r values.

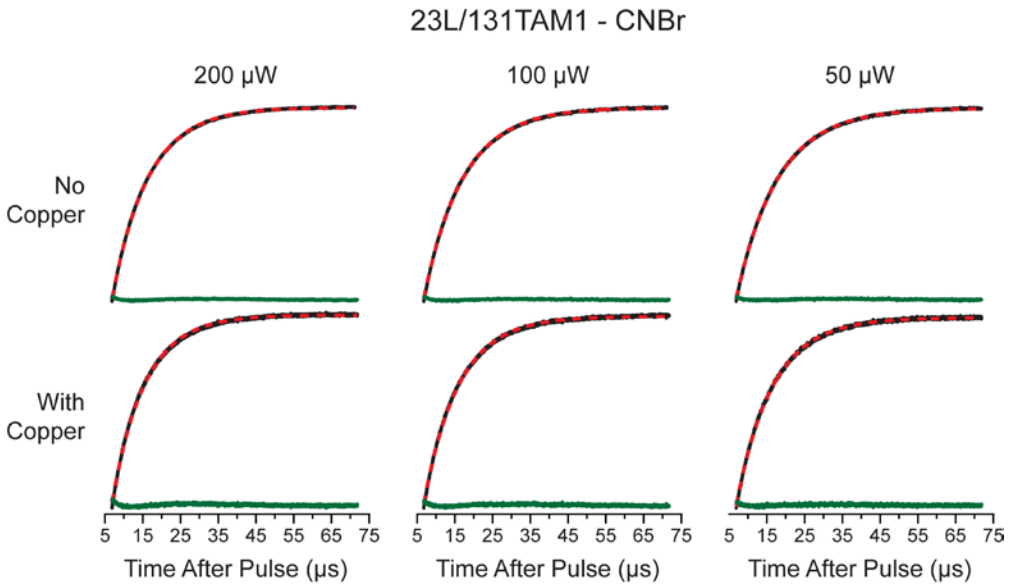

Figure S1. Raw saturation recovery data (black traces), best fit (red dashed traces), and residual (green traces) for the 23L/131TAM1 immobilized on CNBr solid support at three different observe powers. Spectra were obtained for samples in the absence (top) and presence (bottom) of Cu^{2+} and then were globally fit to obtain T_{1s}^0 and r.

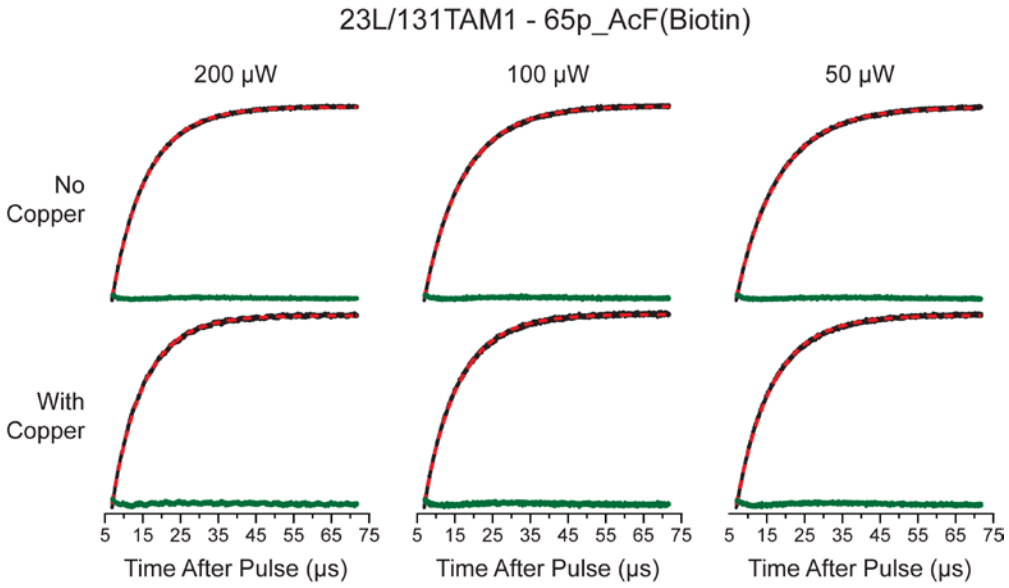

Figure S2. Raw saturation recovery data (black traces), best fit (red dashed traces), and residual (green traces) for the 23L/131TAM1/65p_AcF(Biotin) site-specifically immobilized on streptavidin-coated beads at three different observe powers. Spectra were obtained for samples in the absence (top) and presence (bottom) of Cu^{2+} and then were globally fit to obtain T_{1s}^{0} and r.

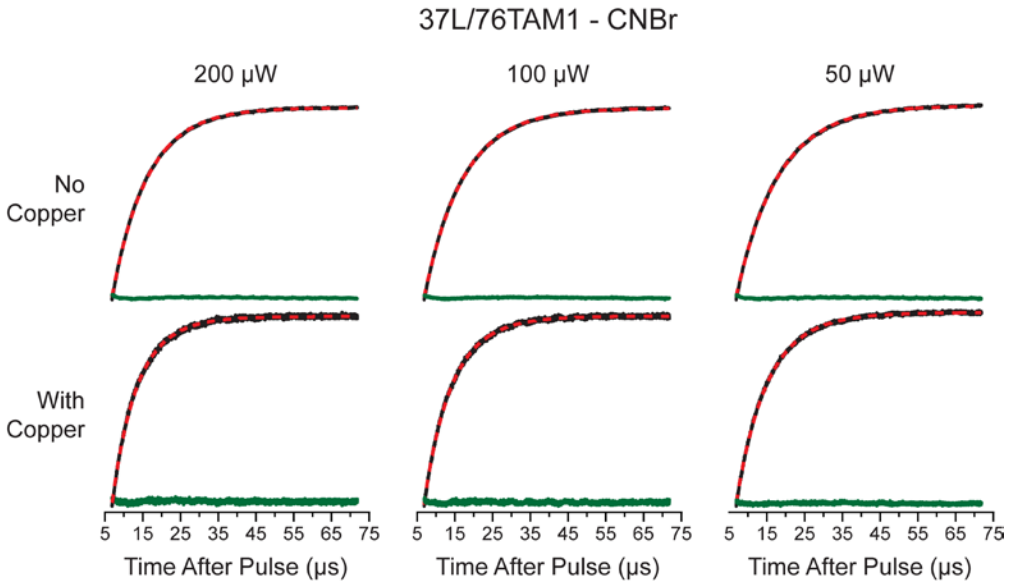

Figure S3. Raw saturation recovery data (black traces), best fit (red dashed traces), and residual (green traces) for the 37L/76TAM1 immobilized on CNBr solid support at three different observe powers. Spectra were obtained for samples in the absence (top) and presence (bottom) of Cu^{2+} and then were globally fit to obtain T_{1s}^{0} and r.

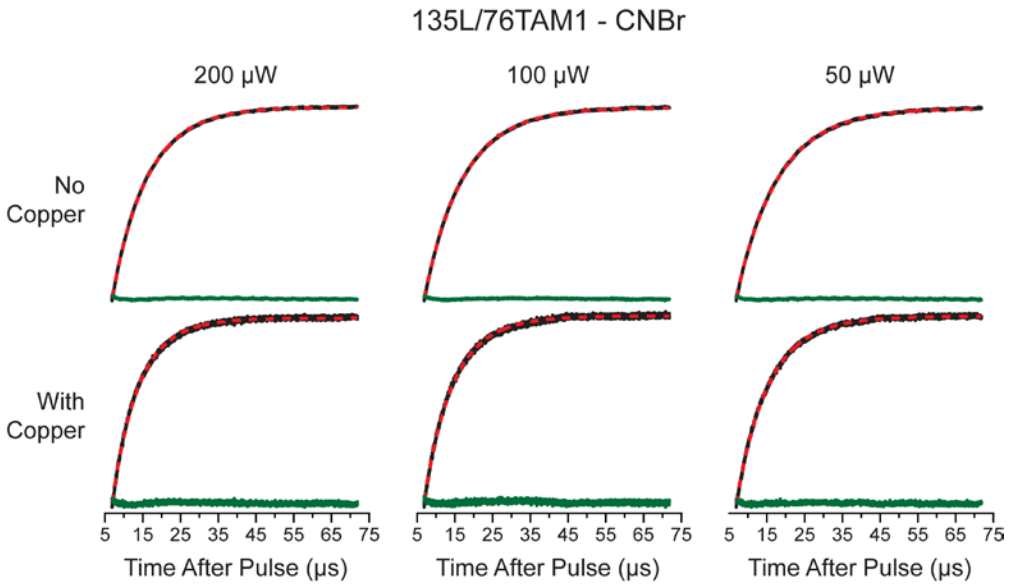

Figure S4. Raw saturation recovery data (black traces), best fit (red dashed traces), and residual (green traces) for the 135L/76TAM1 immobilized on CNBr solid support at three different observe powers. Spectra were obtained for samples in the absence (top) and presence (bottom) of Cu^{2+} and then were globally fit to obtain T_{1s}^{0} and r.

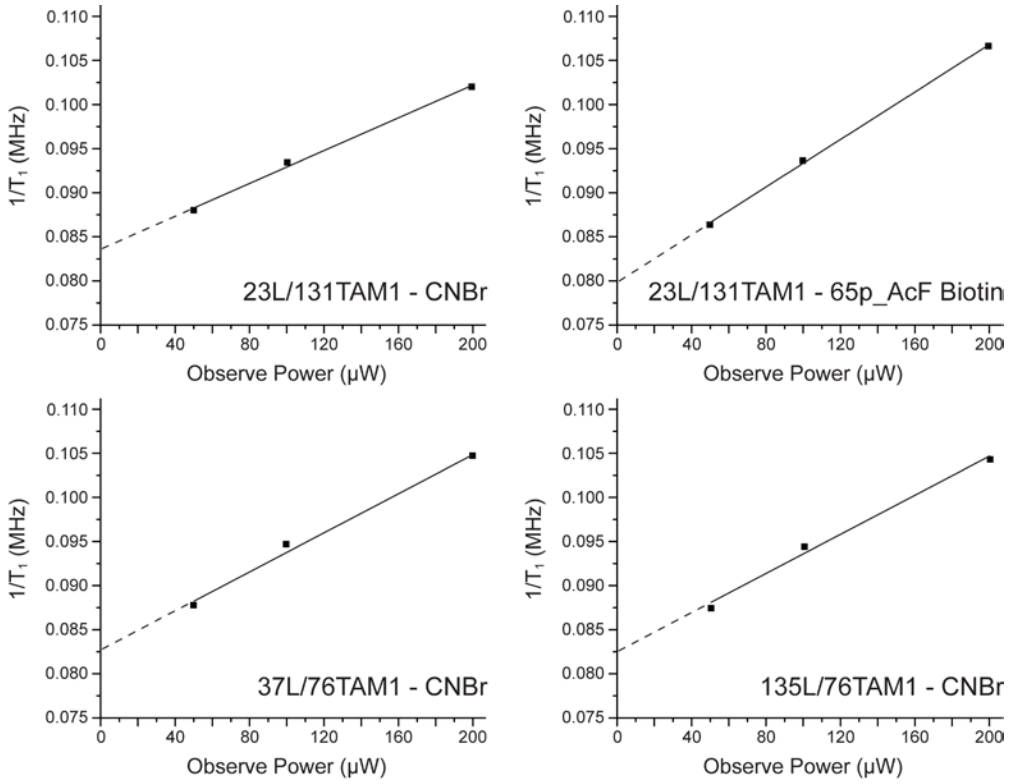

Figure S5. Extrapolation to zero observe power to determine intrinsic T_{1s}^{0}. SR data for each mutant were obtained at three observe powers (50, 100, and 200 µW), and copper-free T_1s, T_{1s}^{0}, were determined by the fitting method described above. Inverse T_1s were plotted versus observe power, yielding an intercept equal to $1/T_{1s,intrinsic}^{0}$.

Table S1. Copper-free T_1s for TAM in 23L/131TAM1 immobilized on CNBr solid support and calculated interspin distances at various observe powers.

Observe Power (μW)	T_{1s}^0 (μs)[a]	Interspin Distance (Å)[a]
200	9.80 (1)	38.7 (1)
100	10.70 (1)	37.5 (1)
50	11.37 (1)	37.0 (1)
0 (*extrapol.*)[b]	11.95 (1)	
Averaged[c]		37.9 (1)

[a] *Errors to last digit given in parentheses.* [b] *Extrapolated value calculated as described above; see Figure S1.* [c] *Average value calculated as weighted by relative errors.*

Table S2. Copper-free T_1s for TAM in 23L/131TAM1/65p_AcF (Biotin) site-specifically immobilized on streptavidin-coated beads and calculated interspin distances at various observe powers.

Observe Power (μW)	T_{1s}^0 (μs)[a]	Interspin Distance (Å)[a]
200	9.38 (1)	39.6 (1)
100	10.68 (1)	37.0 (1)
50	11.58 (1)	36.1 (1)
0 (*extrapol.*)[b]	12.52 (2)	
Averaged[c]		37.7 (1)

[a] *Errors to last digit given in parentheses.* [b] *Extrapolated value calculated as described above; see Figure S1.* [c] *Average value calculated as weighted by relative errors.*

Table S3. Copper-free T_1s for TAM in 37L/76TAM1 immobilized on CNBr solid support and calculated interspin distances at various observe powers.

Observe Power (μW)	T_{1s}^0 (μs)[a]	Interspin Distance (Å)[a]
200	9.57 (1)	30.8 (1)
100	10.58 (1)	31.6 (1)
50	11.41 (1)	33.1 (1)
0 (*extrapol.*)[b]	12.10 (1)	
Averaged[c]		32.6 (1)

[a] *Errors to last digit given in parentheses.* [b] *Extrapolated value calculated as described above; see Figure S1.* [c] *Average value calculated as weighted by relative errors.*

Table S4. Copper-free T_1s for TAM in 135L/76TAM1 immobilized on CNBr solid support and calculated interspin distances at various observe powers.

Observe Power (μW)	T_{1s}^0 (μs)[a]	Interspin Distance (Å)[a]
200	9.56 (1)	32.1 (1)
100	10.58 (1)	32.5 (1)
50	11.40 (1)	33.1 (1)
0 (*extrapol.*)[b]	12.09 (1)	
Averaged[c]		32.8 (1)

[a] *Errors to last digit given in parentheses.* [b] *Extrapolated value calculated as described above; see Figure S1.* [c] *Average value calculated as weighted by relative errors.*

10. Molecular modeling to predict interspin distances between Cu^{2+} and TAM1.

The position of Cu^{2+} in the high affinity peptide was estimated from MD simulations as previously reported [2]. The average coordinates of Cu^{2+} in each MD study were used to compute the Cu^{2+}-TAM distance. The TAM was modeled according to the following: (1) the first dihedral (X_1, about the C_α-C_β bond) was fixed as the same as the native residue at the site [18]. For the cases considered here, X_1 = **m**

(nominally -60°); (2) The fragment -C_α-C_β-S_γ-S_δ- was given to geometry found for a preferred rotamer of R1 at helical sites. This rotamer is determined by backbone-disulfide interactions, and is expected to be the same for TAM1 and R1 that share the common disulfide linkage. Thus, the first three dihedrals of TAM1 were set to {**m, m, m**} [19]. The next five dihedrals of the linker were set to relaxed conformations that resulted in no steric clashes for 135L/76TAM1 and gave essentially perfect agreement with the experimental data for that site; the conformations are {**m, m, t, t, t**}. This single rotamer gave a modeled distance to the Cu^{2+} in excellent agreement, within about an Angstrom, for the three proteins investigated. The models for each are shown in Figure 2 of the main text.

11. Use of the estimated T_{1f} value of 3 ns for Cu^{2+}.

The 3 ns Cu^{2+} relaxation times (T_{1f} and T_{2f}) used in the current study and prior publications [2,20,21] is within the 1-5 ns range reported by the 2001 solution NMR work of Bertini *et al*. [22]. Within this relaxation time range of 1-5 ns, we chose 3 ns for the present analysis as it gave good agreement with distances obtained by modeling, and is thus empirically justified by the results. In principle, the error in absolute distance measurement due to uncertainty in Cu^{2+} T_1 and T_2 relaxation times could be as large as 20%, when the true relaxation time is close to 1 ns (an effect most pronounced for spin labels with long intrinsic spin lattice relaxation times). However, employing this technology with the goal of measuring interspin distance changes due to conformational movements (rather than absolute distances) cancels out this potential uncertainty in measurement.

REFERENCES

1) A.A. Kuzhelev, D.V. Trukhin, O.A. Krumkacheva, R.K. Strizhakov, O.Y. Rogozhnikova, T.I. Troitskaya, M.V. Fedin, V.M. Tormyshev, E.G. Bagryanskaya, Room-temperature electron spin relaxation of triarylmethyl radicals at the X- and Q-bands, *J. Phys. Chem. B* 119 (2015) 13630-13640.
2) Z. Yang, G. Jiménez-Osés, C.J. López, M.D. Bridges, K.N. Houk, W.L. Hubbell, Long-range distance measurements in proteins at physiological temperatures using saturation recovery EPR spectroscopy, *J. Am. Chem. Soc.* 136 (2014) 15356-15365.
3) C.J. López, M.R. Fleissner, Z. Guo, A.K. Kusnetzow, W.L. Hubbell, Osmolyte perturbation reveals conformational equilibria in spin-labeled proteins, *Protein Sci.* 18 (2009) 1637-1652.
4) M.R. Fleissner, E.M. Brustad, T. Kálai, C. Altenbach, D. Cascio, F.B. Peters, K. Hideg, S. Peuker, P.G. Schultz, W.L. Hubbell, Site-directed spin labeling of a genetically encoded unnatural amino acid, *Proc. Nat. Acad. Sci. USA* 106 (2009) 21637-21642.
5) M. Matsumura, J.A. Wozniak, D.P. Sun, B.W. Matthews, Structural studies of mutants of T4 Lysozyme that alter hydrophobic stabilization, *Journal of Biological Chemistry* 264 (1989) 16059-16066.
6) C.J. López, M.R. Fleissner, E.K. Brooks, W.L. Hubbell, Stationary-phase EPR for exploring protein structure, conformation, and dynamics in spin-labeled proteins, *Biochemistry* 53 (2014) 7067-7075.
7) M.R. Fleissner, M.D. Bridges, E.K. Brooks, D. Cascio, T. Kálai, K. Hideg, W.L. Hubbell, Structure and dynamics of a conformationally constrained nitroxide side chain and applications in EPR spectroscopy, *Proc. Nat. Acad. Sci. USA* 108 (2011) 16241-16246.
8) Z. Yang, Y. Liu, P. Borbat, J.L. Zweier, J.H. Freed, W.L. Hubbell, Pulsed ESR dipolar spectroscopy for distance measurements in immobilized spin labeled proteins in liquid solution, *J. Am. Chem. Soc.* 134 (2012) 9950-9952.

9) D.R. Grassetti, J.F. Murray Jr., Determination of sulfhydryl groups with 2,2'- or 4,4'-dithiodipyridine, *Arch. Biochem. Biophys.* 119 (1967) 41-49.
10) M.D. Bridges, K. Hideg, W.L. Hubbell, Resolving conformational and rotameric exchange in spin-labeled proteins using saturation recovery EPR, *Appl. Magn. Reson.* 37 (2010) 363.
11) S.S. Eaton, J. Harbridge, G.A. Rinard, G.R. Eaton, R.T. Weber, Frequency dependence of electron spin relaxation for three S = 1/2 species doped into diamagnetic solid hosts, *Appl. Magn. Reson.* 20 (2001) 151.
12) J.J. Yin, J.S. Hyde, Use of high observing power in electron spin resonance saturation recovery experiments in spin labeled membranes, *J. Chem. Phys.* 91 (1989) 6029.
13) M.T. Lerch, C.J. López, Z. Yang, M.J. Kreitman, J. Horwitz, W.L. Hubbell, Structure-relaxation mechanism for the response of T4 Lysozyme cavity mutants to hydrostatic pressure, *Proc. Nat. Acad. Sci. USA* 112 (2015) E2437-E2446.
14) C.J. López, Z. Yang, C. Altenbach, W.L. Hubbell, Conformational selection and adaptation to ligand binding in T4 Lysozyme cavity mutants, *Proc. Nat. Acad. Sci. USA* 110 (2013) E4306-E4315.
15) D.J. Hirsh, W.F. Beck, J.B. Innes, G.W. Brudvig, Using saturation-recovery EPR to measure distances in proteins: Applications to photosystem II, *Biochemistry* 31 (1992) 532-541.
16) J.S. Hyde, Saturation recovery methodology. In *Time domain electron spin resonance;* L. Kevan, R.N. Schwartz, Eds.; John Wiley & Sons: New York, 1979; pp. 1–30.
17) H. Sato, S.E. Bottle, J.P. Blinco, A.S. Micallef, G.R. Eaton, S.S. Eaton, Electron spin-lattice relaxation of nitroxyl radicals in temperature ranges that span glassy solutions to low-viscosity liquids, *J. Magn. Reson.* 191 (2008) 66-77.
18) D. Toledo-Warshaviak, V. Khramtzov, D. Cascio, C. Altenbach, W.L. Hubbell, Structure and dynamics of an imidazoline nitroxide side chain with strongly hindered internal motion in proteins, *J. Magn. Reson.* 232 (2013) 53-61.
19) M.R. Fleissner, D. Cascio, W.L. Hubbell, Structural origin of weakly ordered nitroxide motion in spin-labeled proteins, *Protein Sci.* 18 (2009) 893-908.
20) J. Voss, W.L. Hubbell, H.R. Kaback, Distance determination in proteins using designed metal ion binding sites and site-directed spin labeling: Application to the lactose permease of *Escherichia coli*, *Proc. Nat. Acad. Sci. USA* 92 (1995) 12300-12303.
21) S. Jun, J.S. Becker, M. Yonkunas, R. Coalson, S. Saxena, Unfolding of alanine-based peptides using electron spin resonance distance measurements, *Biochemistry* 45 (2006) 11666-11673.
22) I. Bertini, C. Luchinat, G. Parigi, Solution NMR of Paramagnetic Molecules: Applications to metallobiomolecules and models. Elsevier Science: New York, 2001; Vol. 2.